Design and Validation of a Device for Mitigating Fluid Microgravity Effects in Biological Research in Canister Spaceflight Hardware

Wayne L. Nicholson[1]*, Patricia Fajardo-Cavazos[1], Caleb Turner[2], Taylor M. Currie[3], Geoffrey Gregory[4], Titel Jurca[3,5] and Mark Weislogel[2†]

[1]Department of Microbiology and Cell Science, University of Florida, Gainesville, FL, United States, [2]Department of Mechanical and Materials Engineering, Portland State University, Portland, OR, United States, [3]Department of Chemistry, University of Central Florida, Orlando, FL, United States, [4]Department of Materials Science and Engineering, University of Central Florida, Orlando, FL, United States, [5]Renewable Energy and Chemical Transformations Cluster, University of Central Florida, Orlando, FL, United States

The major factor influencing the behavior of microbes growing in liquids in space is microgravity. We recently measured the transcriptomic response of the Gram-positive bacterium *Bacillus subtilis* to the microgravity environment inside the International Space Station (ISS) in spaceflight hardware called Biological Research in Canisters-Petri Dish Fixation Units (BRIC-PDFUs). In two separate experiments in the ISS, dubbed BRIC-21 and BRIC-23, we grew multiple replicates of the same *B. subtilis* strain in the same hardware, growth medium, and temperature with matching ground control samples (*npj Micrograv.* 5:1.2019, doi: 10.1038/s41526-018-0061-0). In both experiments we observed similar responses of the transcriptome to spaceflight. However, we also noted that the liquid cultures assumed a different configuration in microgravity (a toroidal shape) compared with the ground control samples (a flat disc shape), leading us to question whether the transcriptome differences we observed were a direct result of microgravity, or a secondary result of the different liquid geometries of the samples affecting, for example, oxygen availability. To mitigate the influence of microgravity on liquid geometry in BRIC canisters, we have designed an insert to replace the standard 60-mm Petri dish in BRIC-PDFU or BRIC-LED sample compartments. In this design, liquid cultures are expected to assume a more disk-like configuration regardless of gravity or its absence. We have: (i) constructed a prototype device by 3D printing; (ii) evaluated different starting materials, treatments, and coatings for their wettability (i.e., hydrophilicity) using contact angle measurements; (iii) confirmed that the device performs as designed by drop-tower testing and; (iv) performed material biocompatibility studies using liquid cultures of *Bacillus subtilis* and *Staphylococcus aureus* bacteria. Future microgravity testing of the device in the ISS is planned.

Keywords: *Bacillus subtilis*, BRIC, capillarity, liquid culture, microgravity

INTRODUCTION

Effective handling of liquids in microgravity and low-acceleration environments is essential for optimal performance of numerous systems in spaceflight such as propulsion, heating/cooling, water purification, and life support. Liquids are often contained within receptacles such as tanks or bottles which also contain air or other gases, constituting two-phase systems. Liquid behavior in microgravity is strongly influenced by liquid wetting and container geometry, as interaction with the container wall is dominated by capillary action (Meseguer et al., 2014), presenting a challenge for controlling the stability and location of the liquid phase within the receptacle. This issue drives the design of liquid containers and handling devices which must operate nominally in microgravity. Management of liquids in microgravity is also of primary importance in Space Biology, where a submerged organism's access to dissolved gases and nutrients is critical. In microgravity, convective heat and mass transfer within fluids is effectively nullified, and mobility of dissolved gases, nutrient and waste solutes becomes dominated by diffusion [reviewed in (Rosenzweig et al., 2014)].

The present study was initiated in response to prior results from spaceflight experiments conducted in the International Space Station (ISS) in Biological Research in Canister (BRIC) hardware. The development of BRIC hardware has been described in detail previously (Wells et al., 2001). Briefly, BRIC hardware samples are contained within five separate compartments called Petri Dish Fixation Units (PDFUs), each of which encloses the bottom of one 60-mm Petri dish, which in turn contains the sample culture (Wells et al., 2001). Originally designed for organisms such as plant seedlings cultivated on semisolid agar media (Wells et al., 2001; Kiss et al., 2007; Kruse et al., 2020), we subsequently introduced modifications in BRIC-PDFU protocols to enable cultivation of microorganisms in liquid media (Fajardo-Cavazos and Nicholson, 2016b), and to date have successfully cultivated the Gram-positive bacteria *Staphylococcus epidermidis, S. aureus,* and *Bacillus subtilis* on three separate missions to the ISS, designated BRIC-18, BRIC-21 and BRIC-23 (Fajardo-Cavazos and Nicholson, 2016b; Fajardo-Cavazos and Nicholson, 2016a; Morrison et al., 2017; Fajardo-Cavazos et al., 2018; Morrison et al., 2019). In each mission, growth was initiated by injection of liquid growth medium into PDFUs. After a growth period, the experiments were terminated by placing the BRIC units inside the onboard −80°C MELFI freezer and maintaining all samples in a frozen state until their return to the laboratory for further analysis (Fajardo-Cavazos and Nicholson, 2016b). In the BRIC-21 and BRIC-23 experiments we measured the transcriptomic response of *B. subtilis* cells to spaceflight (FL) in comparison to parallel ground control (GC) samples (Morrison et al., 2019). We found a total of 91 genes that were significantly differentially expressed in both experiments, 55 exhibiting higher transcript levels in FL samples and 36 showing higher transcript levels in GC samples.

In the BRIC-PDFU system, injection of medium results in the establishment of a 2-phase system consisting of approximately equal volumes of liquid culture and trapped air space; note that this air space provides needed oxygen to the culture, as the PDFUs are otherwise hermetically sealed. Upon return from the ISS, we noted that liquid cultures incubated in the microgravity of FL had assumed a toroidal (ring-shaped) configuration in the Petri dishes (**Figure 1A**), distinctly different from the flat disc-shaped configuration observed in the parallel GC samples incubated at 1 xg (**Figure 1B**) (Morrison et al., 2019). We also noted that among the differentially expressed transcripts in the FL vs. GC samples were a number of oxygen-responsive genes, indicating that GC cultures were receiving less oxygen than FL cultures (Morrison et al., 2019). These results suggested to us that the differential expression of some genes in FL vs. GC samples may be a secondary effect of liquid geometry, hence O_2 availability, and not a primary effect of microgravity (Morrison et al., 2019). To remove this potentially confounding factor from future BRIC-PDFU experiments, in this communication we describe the design, fabrication and testing of a novel Petri dish insert designed to mitigate the effect of liquid geometry in microgravity.

MATERIALS AND METHODS

Bacterial strains, medium, and growth conditions. The *Bacillus subtilis* and *Staphylococcus aureus* strains used in this study are listed in **Table 1** and are stored in our laboratory's strain collection as -70°C frozen glycerol stocks. The liquid medium used for all tests was Trypticase Soy Yeast Extract Glycerol (TSYG) medium containing (per L): tryptone, 15; soytone, 5; NaCl, 5; yeast extract, 3; K_2HPO_4, 2.5; glucose, 2.5; glycerol, 10% (v/v); final pH 7. TSYG medium is the standard medium previously used on the BRIC-18, -21, and -23 missions to the ISS (Fajardo-Cavazos and Nicholson, 2016b). Kanamycin (5 µg/ml final concentration) was included in the *B. subtilis* culture media to maintain plasmid pUB110 (Keggins et al., 1978). For viable counts, serial tenfold dilutions in phosphate-buffered saline (PBS) (Nicholson and Setlow, 1990b) were plated on TSY semisolid medium (i.e., TSYG medium without glycerol and containing 16 g agar per L).

B. subtilis spores were prepared by incubation on Schaeffer Sporulation Medium plates (Schaeffer et al., 1965), purified by water washing (Nicholson and Setlow, 1990b) and heat shocked (80°C, 10 min) to kill unsporulated cells. Purified spores were stored at 4°C in ultrapure water; examination of the preparations by phase-contrast microscopy revealed >99% pure spores with little to no cell debris or vegetative cells. Spores were diluted in sterile water to 10^8 colony-forming units (cfu) per mL and heat-activated (65°C, 20 min) to synchronize germination before use. *S. aureus* cells were prepared by overnight cultivation with shaking in TSY liquid medium at 37°C. Strain UAMS-1 and UAMS-1 Δagr were diluted 1:60 and 1:50, respectively, in fresh TSY medium, yielding a predetermined cell concentration of ~10^8 cfu/ml.

Construction of the modified insert. A modified Petri dish was designed, which is depicted as an image from the resulting STereoLithography (.STL) file (**Figure 2A**). The insert was fabricated from clear polycarbonate, sanded, and coated with a layer of clear-coat spray polyurethane to increase its
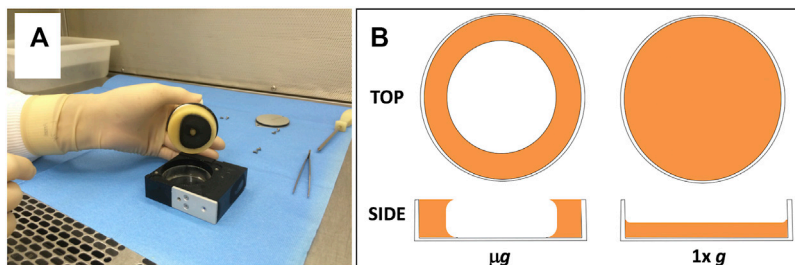
FIGURE 1 | (A) Photograph showing frozen liquid culture being removed from PDFU after BRIC-21 spaceflight mission. Note toroidal-shaped culture adhering to the PDFU manifold and valve; empty 6-cm Petri dish bottom can be seen inside the PDFU chamber. **(B)** Schematic of differing liquid geometries of cultures in Petri dishes in microgravity (μg, left) and Earth-normal gravity (1 xg, right). Both top views and side views are shown. Side views represent a section taken from the center of each dish.

TABLE 1 | Bacterial strains used in this study.

Strain (WN strain number)	Genotype or phenotype	References and source
Bacillus subtilis (WN112)	Strain 168 carrying plasmid pUB110; Km^R	(Nicholson and Setlow, 1990a)
Staphylococcus aureus UAMS-1 (WN1578)	Wild-type clinical isolate	Gillaspy et al. (1995) K.C. Rice
Staphylococcus aureus UAMS-1 Δagr (WN1680)	Strain UAMS-1 carrying a deletion of the *agr* gene	K.C. Rice
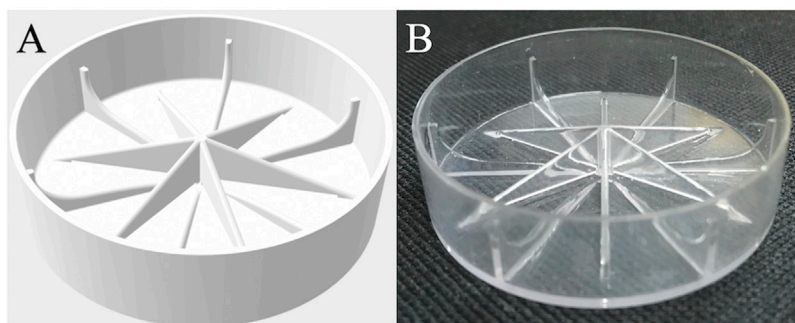
FIGURE 2 | (A) Graphic representation of modified Petri dish bottom designed to mitigate microgravity effects (.STL file). **(B)** Actual modified dish fabricated by 3D printing and coated with polyurethane.

hydrophilicity (**Figure 2B**). Insert fabrication was conducted by a commercial 3D printing service (3D Systems, https://www.3dsystems.com/). Due to the expense involved in using the modified dishes for testing purposes, we built proxies from polycarbonate coupons (98 mm × 40 mm) supplied by 3D Systems by spray coating them with polyurethane (CRC Seal Coat Clear Urethane Coating, CRC Industries, Warminster, PA).

Atomic Layer Deposition (ALD). To further increase hydrophilicity, plastic inserts were coated with amorphous aluminum oxide (Al_2O_3) to various thicknesses using atomic layer deposition (ALD). ALD was performed using a CTECHnano Play Series thermal ALD reactor at a chamber temperature of 100°C, and inlet and outlet temperatures of 90°C. Low temperature ALD was used to maintain the integrity of the polycarbonate inserts. The precursors, trimethylaluminum (TMA) and water (H_2O), were

alternatively pulsed for 250 msec, followed by a 2 s residence time, and 20 s purge each. This recipe was repeated for 15, 50, and 100 cycles to deposit an estimated thickness of 1.5, 5, and 10 nm of Al_2O_3, respectively.

Treatment of Aluminum PDFU manifold valve to increase its hydrophobicity. In prior spaceflight experiments we observed that frozen toroidal-shaped cultures made contact with, and adhered to, the black anodized aluminum manifold valve positioned above the dish (**Figure 1A**). Therefore, we reasoned that increasing the hydrophobicity of the manifold would discourage liquid accumulation on the manifold surface. To test this notion by contact angle measurements, we constructed proxies consisting of 76 mm × 25 mm (3″ × 1″) rectangular black anodized aluminum coupons (Custom Engraving Plates, https://customengravingplates.com/). The protective film was removed from the virgin face of each

coupon and they were coated on the virgin side by spray application of a commercial automotive water-repellent coating (Mothers CMX Ceramic Spray Coating, Mothers, Huntington Beach, CA) followed by buffing and curing per the manufacturer's recommendations.

Contact angle measurements. Hydrophobicity or hydrophilicity of surfaces was determined by contact angle measurements. The contact angle experiments were performed using a contact angle goniometer (Ossila, Sheffield, United Kingdom) and vendor-supplied software. Contact angles of ultra-pure deionized water and sterile TSYG medium on each surface were measured. In all cases measurements were obtained using 5 µL droplets of each liquid. In one set of experiments, droplets were deposited onto either a plain anodized aluminum coupon or an anodized aluminum coupon previously coated with CMX ceramic automotive spray. In a separate set of experiments, droplets of each solution were deposited onto the polycarbonate coupons spray coated with polyurethane and either not coated or additionally coated by ALD with 1.5, 5, or 10 nm of Al_2O_3.

Measurements were performed multiple times with each drop placed in a new spot. As needed, the previous drop was blotted dry with a Kimwipe before proceeding with the next. A 10-s video at five frames per second was taken of each drop, and the contact angles at the start and end of each video were measured within the software. The average of the angles on the left and right sides of each drop was found, and these were averaged for each of the samples measured. Numbers of individual data points for each dataset varied from $n = 6$–8 (aluminum coupons) to $n = 14$–31 (plastic coupons).

Biocompatibility testing. For testing of biocompatibility with Al_2O_3, polycarbonate coupons were cut into equal thirds, and each third was placed into the bottom of a sterile 6-cm Petri dish (Falcon Cat. No. 1007). *B. subtilis* spores or *S. aureus* cells ($\sim 10^7$) were spotted onto the surface of each coupon and air-dried for 24–48 h on the laboratory bench at ambient conditions ($\sim 23°C$, $\sim 40\%$ relative humidity), protected from light. TSYG liquid medium (8.5 ml) was pipetted into each dish and the plates incubated for 25 h at 23°C, mimicking the conditions used in the BRIC-21 and BRIC-23 space flight experiments (Fajardo-Cavazos and Nicholson, 2016b). After incubation, adherent cells were dislodged from each coupon surface by rubbing with a sterile disposable cell scraper (Cat. No. 179693, 23-cm, Thermo Fisher Scientific, Rochester NY). Cultures were transferred to sterile 15-ml conical screw-cap tubes and vortexed vigorously for 10 s to further homogenize cell suspensions. Aliquots were removed from samples and viable counts determined as described above.

For testing biocompatibility with CMX, aluminum coupons were placed into sterile 10-cm Petri dishes and $\sim 10^7$ *B. subtilis* spores or *S. aureus* cells were spotted on each coupon and air-dried. Because CMX-coated coupons repelled liquid in Petri dishes, all coupons were transferred to sterile 50-ml screw-cap centrifuge tubes for testing. Liquid TSYG medium (25 ml) was added to each tube, to replicate the approximate liquid-to-air ratio in PDFUs, and tubes were inverted several times to ensure contact of cells with medium. Tubes were incubated for 25 h at 23°C, then tubes were vortexed and inverted several times to ensure homogeneous cell resuspension. Aliquots were removed from samples and viable counts determined as described above.
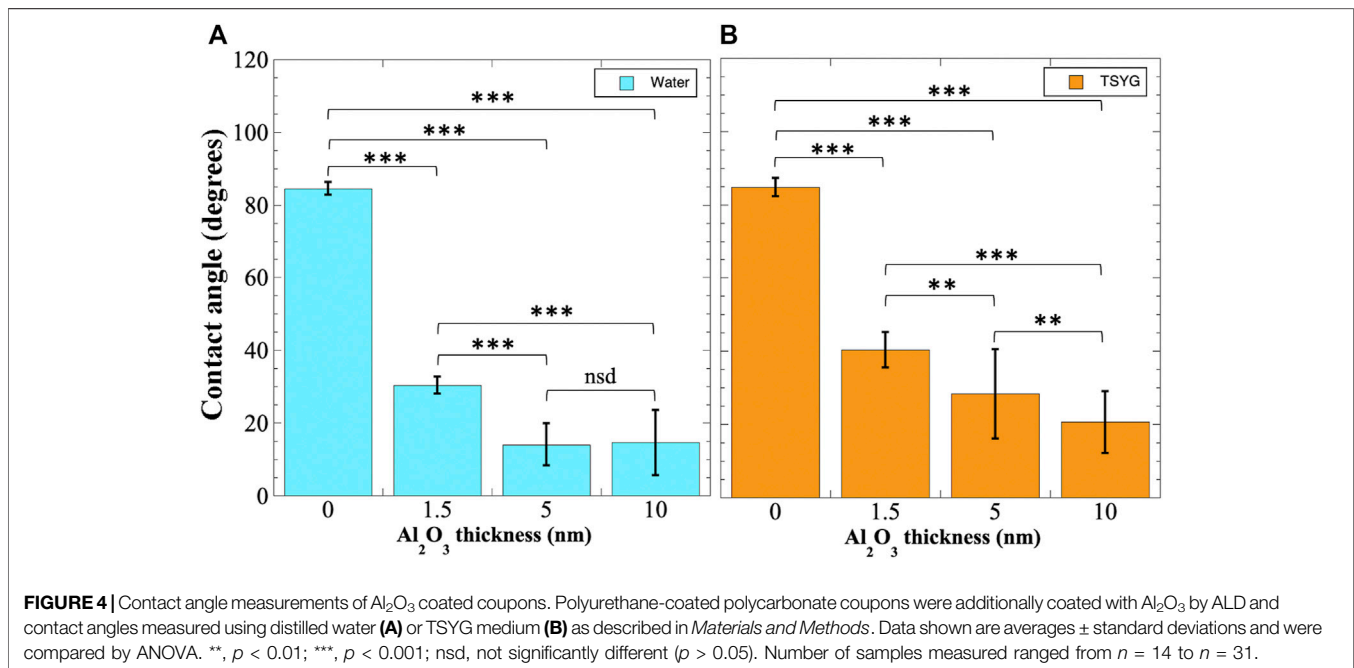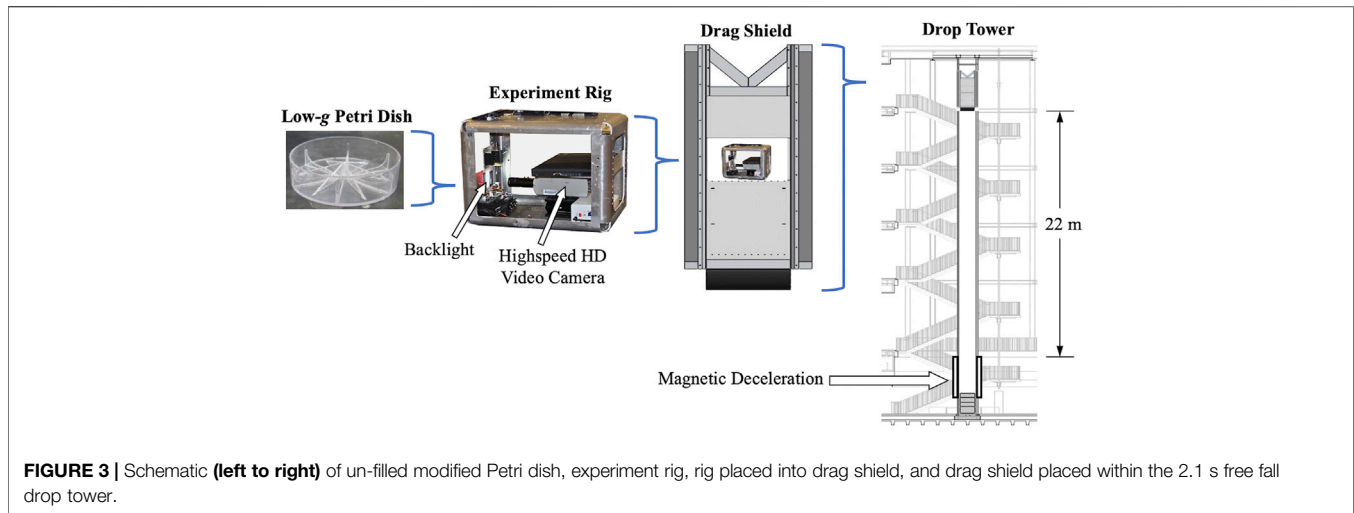
Drop tower testing. Terrestrial low-*g* proof of concept testing was accomplished using the Dryden Drop Tower located at Portland State University, which has been described in detail previously (Wollman et al., 2016; Wollman and Weislogel, 2013). The 22 m tall tower provides approximately 2.1 s of free fall where experiments experience a near weightless state with maximum local accelerations on the order of 10^{-4} g_0. A generalized schematic of the modified Petri dish insert, experiment rig, rig placed into drag shield, and drag shield placed within the drop tower is provided in **Figure 3** with the basic components labeled. A Panasonic WX970 HD camcorder was used to record the fluid interface response to the step-reduction in gravitational magnitude and the following quasi steady state fluid configuration achieved. Video recordings were taken at a rate of 120 frames per second with a resolution of $3840 \times 2,160$ pixels (4K). Video data was then converted to still frame images and qualitatively analyzed using the open source image analysis software FIJI (Schindelin et al., 2012). Testing was performed for each sample at two distinct fluid interface initial configurations, flat and tilted ($\sim 6°$ off horizontal).

Statistics. Outlier data points in contact angle measurement datasets were identified using an online calculator (https://miniwebtool.com/outlier-calculator/) and discarded. Data sets were tested for Normality using the Shapiro-Wilks online calculator (https://www.statskingdom.com/320ShapiroWilk.html) and compared by Analysis of Variance (ANOVA) using the statistics tool included in the graphics program Kaleidagraph version 4.5.4 (Synergy Software, Reading, PA).
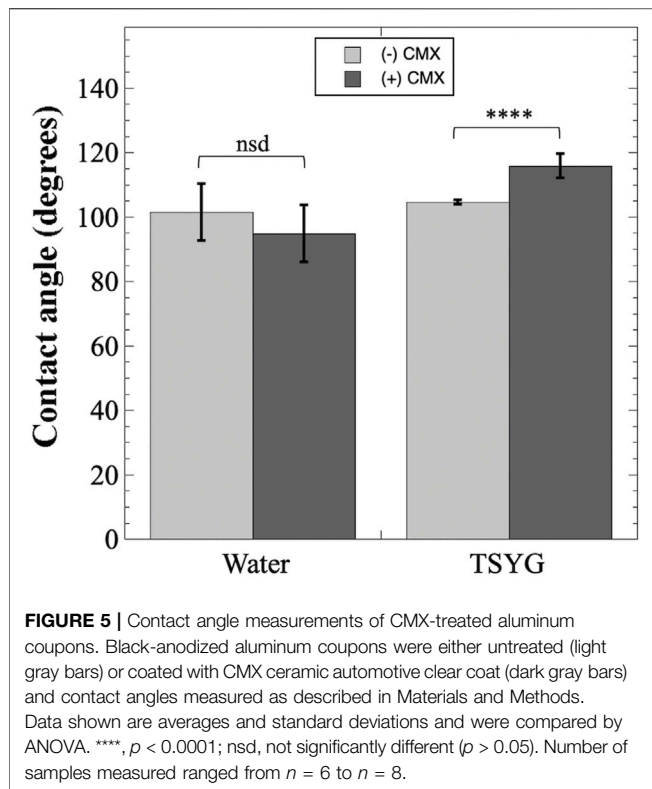
RESULTS AND DISCUSSION

The modified Petri dish insert. We designed and constructed a modified Petri dish insert intended to mitigate the effect of microgravity on liquid configuration in BRIC hardware (**Figure 2**). The particular geometry of the insert borrows from vane structures commonly employed in liquid fuel receptacles aboard spacecraft (Collicott and Weislogel, 2002). In this case, the desire was to establish a global energy-minimizing liquid surface configuration that most nearly replicates the configuration of liquid within a Petri dish on Earth. The tapering radial vanes add wetted surface area and interconnected interior corners to attempt to meet this objective (**Figure 2**). Procedural and geometric complications are understood by the non-ideal manner by which the fluid is injected into the cell, and by a floating disc-like manifold (**Figure 1A**) (Wells et al., 2001).

To increase the wettability (i.e., hydrophilicity) of the insert surfaces, we additionally coated them with Al_2O_3 using ALD. We estimated that the final thicknesses of Al_2O_3 coatings on polyurethane-coated polycarbonate coupons and inserts deposited by ALD to be 1.5, 5, and 10 nm. However, due to the amorphous nature of the substrate material, the actual resulting thickness of Al_2O_3 coatings cannot be measured

FIGURE 3 | Schematic **(left to right)** of un-filled modified Petri dish, experiment rig, rig placed into drag shield, and drag shield placed within the 2.1 s free fall drop tower.

FIGURE 4 | Contact angle measurements of Al_2O_3 coated coupons. Polyurethane-coated polycarbonate coupons were additionally coated with Al_2O_3 by ALD and contact angles measured using distilled water **(A)** or TSYG medium **(B)** as described in *Materials and Methods*. Data shown are averages ± standard deviations and were compared by ANOVA. **, $p < 0.01$; ***, $p < 0.001$; nsd, not significantly different ($p > 0.05$). Number of samples measured ranged from $n = 14$ to $n = 31$.

directly. Our estimates of Al_2O_3 film thicknesses were thus based off controls monitoring growth of Al_2O_3 layers on flat Si wafers using spectroscopic ellipsometry (data not shown). The resulting Al_2O_3 thickness on polycarbonate will largely be influenced by the initial rate of nucleation on the polyurethane top surface, measurement of which is beyond the scope of this study. Nonetheless, measurements on Si wafers were commensurate with a ~0.1 nm/cycle increase in thickness, in line with the general literature (Strempel et al., 2018). As ALD is a layer by layer, conformal thin-film growth process (George, 2010), we reasoned that the general thicknesses of Al_2O_3 on polycarbonate would be of a similar order of magnitude to those measured on Si wafer during recipe development.

Contact angle measurements. To assess the hydrophilicity of Al_2O_3-coated plastic surfaces, we performed contact angle measurements on proxy coupons as described in *Materials and Methods*. First, we measured the effect on the resulting contact angle of additionally coating the polyurethane-coated polycarbonate surfaces with 1.5, 5, or 10 nm of Al_2O_3. Contact angles of both sterile distilled water and sterile TSYG medium droplets were measured (**Figure 4**). When water droplets were measured, it was observed that polyurethane-coated coupons were only slightly hydrophilic, with an average contact angle of 84.5 ± 1.8° (**Figure 4A**). Application of 1.5 and 5 nm Al_2O_3 coatings dramatically reduced the contact angle to 30.4 ± 2.4° and 14.1 ± 5.8°, respectively; however, application of 10 nm Al_2O_3 did not further reduce the contact angle significantly (**Figure 4A**).

FIGURE 5 | Contact angle measurements of CMX-treated aluminum coupons. Black-anodized aluminum coupons were either untreated (light gray bars) or coated with CMX ceramic automotive clear coat (dark gray bars) and contact angles measured as described in Materials and Methods. Data shown are averages and standard deviations and were compared by ANOVA. ****, $p < 0.0001$; nsd, not significantly different ($p > 0.05$). Number of samples measured ranged from $n = 6$ to $n = 8$.

When TSYG medium droplets were measured, a similar pattern of contact angle reduction was seen. Untreated polyurethane-coated polycarbonate coupons were again slightly hydrophilic, exhibiting an average contact angle of $84.7 \pm 2.5°$ (**Figure 4B**). However, in the case of TSYG medium, a progressive and significant increase in surface hydrophilicity was observed on surfaces coated with 1.5, 5, and 10 nm Al_2O_3, with contact angles reduced to $40.4 \pm 4.9°$, $28.3 \pm 12.2°$, and $20.7 \pm 8.4°$, respectively (**Figure 4B**). Because the growth medium used in BRIC-PDFU experiments is TSYG, it appeared that coating of the interior surfaces of the insert with 10 nm Al_2O_3 would provide optimal hydrophilic conditions for maintaining proper liquid geometry in microgravity.

To discourage accumulation of liquid on the black-anodized aluminum manifold surfaces in PDFUs (**Figure 1**), we explored coating aluminum proxy coupons with the hydrophobic automotive ceramic coating CMX. Hydrophobicity of the resulting surfaces was assessed using contact angle measurements (**Figure 5**). The untreated aluminum surface was found to be slightly hydrophobic to water, with an average contact angle of $101.4 \pm 9.8°$, and treatment with CMX did not significantly alter the contact angle (**Figure 5**). When TSYG medium was tested, the untreated coupons were again found to be slightly hydrophobic with an average contact angle of $104.6 \pm 0.9°$ (**Figure 5**); treatment with CMX was observed to increase the hydrophobicity significantly, with a resulting contact angle of $115.9 \pm 4.5°$ (**Figure 5**).

Biocompatibility of materials. Testing the materials used in spaceflight hardware for their compatibility with cells and growth media is an important consideration in the design and conduct of spaceflight missions (Schultz et al., 2012; Nicholson and Ricco, 2020). In standard BRIC-PDFU hardware, cells and media are in contact with various materials including the black polycarbonate PDFU itself, the black-anodized aluminum manifold, polystyrene Petri dish bottoms, and Teflon and stainless-steel valve components. These materials have all been thoroughly tested and found to be biocompatible with *B. subtilis*, *S. aureus*, and *S. epidermidis* bacterial cells grown in liquid TSYG medium (Fajardo-Cavazos and Nicholson, 2016b). However, in production of the modified Petri dish insert and modified manifold described here additional materials have been added, specifically Al_2O_3 and CMX automotive clear coat. We therefore tested these materials for their biocompatibility.

Regarding Al_2O_3, a prior publication had reported no ill effects on *Escherichia coli* or *B. subtilis* cells after direct exposure to Al_2O_3 nanoparticles (Sadiq et al., 2015). We tested the biocompatibility of Al_2O_3 coatings on *B. subtilis* strain WN112 and *S. aureus* strains WN1578 and WN1680 grown in direct contact with polycarbonate coupons coated with polyurethane and Al_2O_3 (**Figure 6**). Neither germination nor growth of *B. subtilis* strain WN112 was significantly affected by contact with Al_2O_3 coatings of 1.5, 5, or 10 nm thickness compared to the control coupons not coated with Al_2O_3 (**Figure 6A**). However, growth of *S. aureus* strains WN1578 and WN1680 was inhibited by 1 and 1.6 orders of magnitude, respectively, after exposure to coupons coated with 10 nm Al_2O_3 (**Figure 6B**). We therefore concluded that the Al_2O_3 coating used in the inserts was biocompatible with *B. subtilis* but not with *S. aureus* cells.

Regarding CMX, we compared the biocompatibility of uncoated aluminum coupons with that of CMX-coated coupons (**Figure 7**). Viability of *B. subtilis* WN112 cells was found to be slightly (~1.2-fold) but significantly higher on CMX-coated coupons than on uncoated control coupons (**Figure 7**). When *S. aureus* cells were tested, we noted that the difference in viable titers of wild-type *S. aureus* WN1578 cells was not significantly different between the control and CMX-treated coupons (**Figure 7**). However, in the case of *S. aureus* WN1680 cells containing a deletion of the *agr* gene (**Table 1**), exposure of cells to CMX coated coupons resulted in a significant reduction in titer by a factor of ~2.9 fold, from $8.9 \pm 2.6 \times 10^8$ to $3.1 \pm 1.7 \times 10^8$ (**Figure 7**). The *agr* locus is an important quorum sensing regulator for numerous biofilm- and virulence-associated functions in *S. aureus* (Wang and Muir, 2016); apparently, inactivation of *agr* also affects sensitivity to CMX (**Figure 7**).

In the process of choosing a hydrophobic coating, we selected CMX over the more traditional polytetrafluoroethylene PTFE (i.e., Teflon™) due to concerns about the negative health and environmental effects of PTFE and its precursors, per- and polyfluoroalkyl substances (PFAS) (Lohmann et al., 2020); at present, no such concerns are reported for the hydrophobic active ingredient in CMX, octamethylcyclotetrasiloxane (D_4) (Franzen et al., 2017). The hydrophobicity of PTFE-coated aluminum surfaces has been measured previously both in 1 x*g* and reduced gravity, with contact angles reported in the literature in the range of 110–115° (Diana et al., 2012; Taft
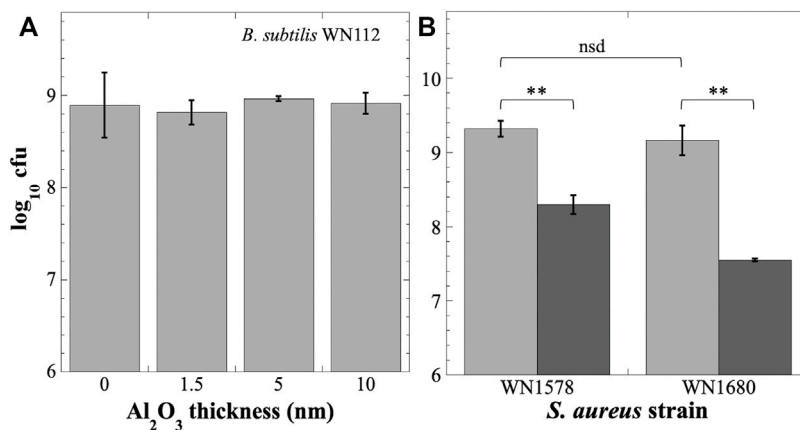
FIGURE 6 | Testing Al$_2$O$_3$ coating for biocompatibility with *B. subtilis* **(A)** or *S. aureus* **(B)** after growth on polyurethane-coated polycarbonate coupons. **(A)** Titer of *B. subtilis* strain WN112 on coupons coated with Al$_2$O$_3$ at the indicated thicknesses. Titers were not significantly different (nsd) ($p > 0.05$, ANOVA, $n = 3$). **(B)** Titers of *S. aureus* strains WN1578 and WN1680 on uncoated coupons (light gray bars) or coupons coated with 10 nm Al$_2$O$_3$ (dark gray bars). **, $p < 0.01$; nsd, $p > 0.05$ (ANOVA, $n = 3$).
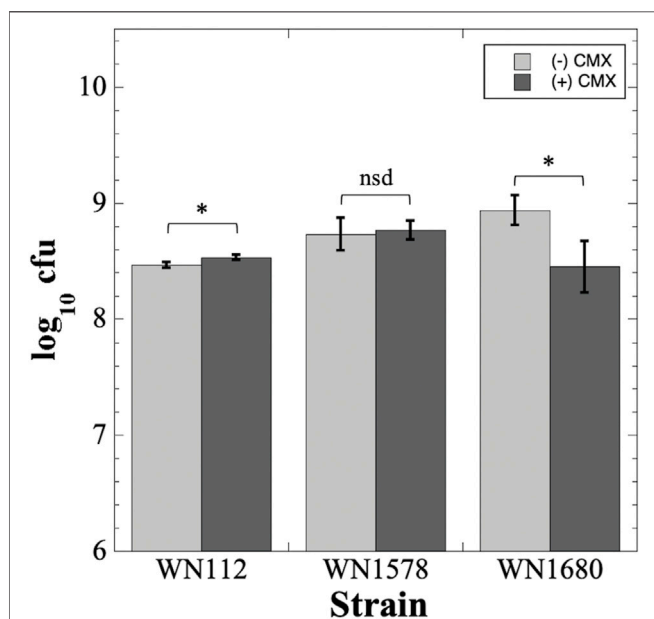
FIGURE 7 | Testing CMX for biocompatibility with *B. subtilis* WN112 and *S. aureus* WN1578 and WN1680 cells. Cell titers on uncoated aluminum coupons (light gray bars) or CMX-coated coupons (dark gray bars) were determined as described in *Materials and Methods* and are depicted as averages ± standard deviations. *, $p < 0.05$; nsd, $p > 0.05$ (ANOVA, $n = 3$).

et al., 2014). Using TSYG medium on CMX-coated aluminum we measured contact angles of $115.9 \pm 4.5°$ (**Figure 5**), essentially identical to PTFE-coated aluminum. These observations highlight the importance of biocompatibility testing whenever a new material or a new bacterial strain is considered for spaceflight.

Drop tower testing of inserts. The performance of inserts in mitigating microgravity effects was assessed by drop tower testing. We fabricated inserts using four material configurations: uncoated polycarbonate (PC), polycarbonate coated with polyurethane (PC + PU), polycarbonate coated with Al$_2$O$_3$ (PC + Al), and polycarbonate coated with both polyurethane and Al$_2$O$_3$ (PC + PU + Al) as outlined in **Table 2**. Each configuration was subjected to two drop tower tests, one in the horizontal (flat) position and one tilted by ~6° from horizontal. Video files documenting the ~2.1-s free fall experiments for each configuration are listed in **Table 2** and can be found in the **Supplementary Material**.

In the flat orientation, both the PC and PC + PU inserts maintained liquid TSYG in the bottom of the insert as designed, with little to no change in liquid geometry (**Supplementary Movies 1, 3**). In the inserts containing Al$_2$O$_3$ coating (PC + Al and PC + PU + Al) in the flat orientation, some "creeping" of the liquid TSYG up the sides of the inserts was noted during free fall, likely due to the increased hydrophilicity imparted by the Al$_2$O$_3$ coating (**Supplementary Movies 5, 7**). From these tests, it appeared that the PC and PC + PU samples performed best in maintaining the liquid in a 1x g geometry, as long as the liquid started out in that geometry. However, in the drop tower tests, liquid TSYG is already present in its final 1 xg orientation. In contrast, in an experiment in the PDFU, growth is initiated by injection of a stream of TSYG medium into the insert; the liquid migrates to its final equilibrium position, not merely maintaining its initial geometry. To emulate this situation, we performed a series of drop tower tests in which the inserts were tilted ~6° off horizontal, to visualize migration of the TSYG medium from its initial geometry to its final geometry over the 2.1 s of lowered gravity. We observed that the PC and PC + PU inserts failed to migrate to their new equilibrium position during the period of lowered gravity (**Supplementary Movies 2, 4**). However, in the inserts coated with Al$_2$O$_3$ it was observed that the liquid TSYG readily migrated to its final tilted

TABLE 2 | Information used for drop-tower testing of inserts.

Polycarbonate	Polyurethane coated	Al$_2$O$_3$ coated	Position	Supplementary movie file
X	-	-	Flat	1-PCflat.MP4
X	-	-	Tilted	2-PCtilt.MP4
X	X	-	Flat	3-PC + PUflat.MP4
X	X	-	Tilted	4-PC + PUtilt.MP4
X	-	X	Flat	5-PC + Al2O3flat.MP4
X	-	X	Tilted	6-PC + Al2O3tilt.MP4
X	X	X	Flat	7-PC + PU + Al2O3flat.MP4
X	X	X	Tilted	8-PC + PU + Al2O3tilt.MP4
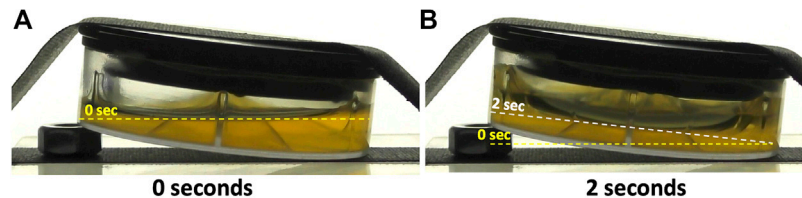
FIGURE 8 | Individual frames of drop tower experiment taken from **Supplementary Movie 8**-PC + PU + Al2O3tilt.MP4 taken at 0 s **(A)** and 2 s **(B)**. Horizontal meniscus at 0 s is denoted by the yellow dashed lines in panels **(A)** and **(B)**, and the final tilted meniscus, parallel with the bottom of the insert, is denoted by the white dashed line in panel **(B)**

position within the insert during the 2.1 s period of lowered gravity (**Supplementary Movies 6, 8**); again, some "creeping" of liquid up the sides of the dish was noted. Failure of the PC and PC + PU inserts to migrate to the tilted position within 2.1 s could be due to insufficient time in the drop tower; this possibility could be tested further before spaceflight by using a platform providing for longer times in lowered gravity, such as a parabolic flight which can generate 10^{-2}–$10^{-3}g$ for up to ~20 s, or a suborbital rocket which can generate $<10^{-5}g$ for a few minutes (Wells et al., 2001; Kiss et al., 2007; NRC, 2011; Rosenzweig et al., 2014; Fajardo-Cavazos and Nicholson, 2016b; Kruse et al., 2020).

In **Figure 8** we present "before" **(A)** and "after" **(B)** frames of the drop tower test of the PC + PU + Al insert, taken from **Supplementary Movie 8**. At 0 s, the liquid meniscus is parallel to the floor of the chamber and tilted by ~6° with respect to the insert itself (**Figure 8A**). At 2 s, just prior to termination of the free-fall period, the meniscus has migrated to be parallel with the bottom of the insert and is now tilted by ~6° with respect to the floor of the chamber (**Figure 8B**). Although some "creeping" of liquid up the walls of the insert is seen in lowered gravity, it is evident that the bulk of the liquid remains in the bottom of the dish (**Figure 8B**). These results suggest that liquid injected under microgravity conditions into the PDFU containing the PC + PU + Al insert would be encouraged, by the vane design and hydrophilic coating, to migrate into the bottom of the dish and remain there for the duration of the experiment if left undisturbed.

In this communication we describe the design, construction, and testing of a new insert to mitigate microgravity effects on liquid cultures of bacteria cultivated in BRIC-PDFU hardware. The insert appears to function as designed in maintaining liquid culture medium in the bottom of the modified Petri dish in

microgravity, at least over the short 2.1-s duration of the drop tower tests. Our results also showed that biocompatibility testing is an important component of pre-flight characterization of the system. Long-duration testing of the inserts' performance in the microgravity environment of the ISS is planned using *B. subtilis* and *S. aureus*. We anticipate that space flights using additional microbial species will further prove the general utility of this device.

DATA AVAILABILITY STATEMENT

The raw data supporting the conclusions of this article will be made available by the authors, without undue reservation.

AUTHOR CONTRIBUTIONS

WN and MW conceived the study. All authors performed the experiments and wrote the manuscript.

FUNDING

ACKNOWLEDGMENTS

The authors thank Kelly Rice for generous donation of strains UAMS-1 and UAMS-1Δagr, as well as Craig Kundrot and Howard Levine of NASA for their support of this project since its inception.

REFERENCES

Collicott, S. H., and Weislogel, M. M. (2002). "Modeling of the Operations of the VTRE Propellant Management Device," in 38th AIAA/ASME/SAE/ASEE Joint Propulsion Conference and Exhibit, Indianapolis, July 7–10, 2002.

Diana, A., Castillo, M., Brutin, D., and Steinberg, T. (2012). Sessile Drop Wettability in Normal and Reduced Gravity. Microgravity Sci. Technol. 24 (3), 195–202. doi:10.1007/s12217-011-9295-0

Fajardo-Cavazos, P., Leehan, J. D., and Nicholson, W. L. (2018). Alterations in the Spectrum of Spontaneous Rifampicin-Resistance Mutations in the Bacillus subtilis rpoB Gene after Cultivation in the Human Spaceflight Environment. Front. Microbiol. 9, 192. doi:10.3389/fmicb.2018.00192

Fajardo-Cavazos, P., and Nicholson, W. L. (2016a). Cultivation of Staphylococcus epidermidis in the Human Spaceflight Environment Leads to Alterations in the Frequency and Spectrum of Spontaneous Rifampicin-Resistance Mutations in the rpoB Gene. Front. Microbiol. 7, 999. doi:10.3389/fmicb.2016.00999

Fajardo-Cavazos, P., and Nicholson, W. L. (2016b). Establishing Standard Protocols for Bacterial Culture in Biological Research in Canisters (BRIC) Hardware. Gravit. Space Res. 4 (2), 58–69. doi:10.2478/gsr-2016-0013

Franzen, A., Greene, T., Van Landingham, C., and Gentry, R. (2017). Toxicology of octamethylcyclotetrasiloxane (D 4). Toxicol. Lett. 279 (Suppl. 1), 2–22. doi:10.1016/j.toxlet.2017.06.007

George, S. M. (2010). Atomic Layer Deposition: an Overview. Chem. Rev. 110 (1), 111–131. doi:10.1021/cr900056b

Gillaspy, A. F., Hickman, S. G., Skinner, R. A., Thomas, J. R., Nelson, C. L., and Smeltzer, M. S. (1995). Role of the Accessory Gene Regulator (agr) in Pathogenesis of Staphylococcal Osteomyelitis. Infect. Immun. 63 (9), 3373–3380. doi:10.1128/iai.63.9.3373-3380.1995

Keggins, K. M., Lovett, P. S., and Duvall, E. J. (1978). Molecular Cloning of Genetically Active Fragments of Bacillus DNA in Bacillus subtilis and Properties of the Vector Plasmid pUB110. Proc. Natl. Acad. Sci. 75 (3), 1423–1427. doi:10.1073/pnas.75.3.1423

Kiss, J. Z., Kumar, P., Bowman, R. N., Steele, M. K., Eodice, M. T., Correll, M. J., et al. (2007). Biocompatibility Studies in Preparation for a Spaceflight experiment on Plant Tropisms (TROPI). Adv. Space Res. 39 (7), 1154–1160. doi:10.1016/j.asr.2006.12.017

Kruse, C. P. S., Meyers, A. D., Basu, P., Hutchinson, S., Luesse, D. R., and Wyatt, S. E. (2020). Spaceflight Induces Novel Regulatory Responses in Arabidopsis Seedling as Revealed by Combined Proteomic and Transcriptomic Analyses. BMC Plant Biol. 20 (1), 237. doi:10.1186/s12870-020-02392-6

Lohmann, R., Cousins, I. T., DeWitt, J. C., Glüge, J., Goldenman, G., Herzke, D., et al. (2020). Are Fluoropolymers Really of Low Concern for Human and Environmental Health and Separate from Other PFAS? Environ. Sci. Technol. 54 (20), 12820–12828. doi:10.1021/acs.est.0c03244

Meseguer, J., Sanz-Andrés, A., Pérez-Grande, I., Pindado, S., Franchini, S., and Alonso, G. (2014). Surface Tension and Microgravity. Eur. J. Phys. 35 (5), 055010. doi:10.1088/0143-0807/35/5/055010

Morrison, M. D., Fajardo-Cavazos, P., and Nicholson, W. L. (2019). Comparison of Bacillus subtilis Transcriptome Profiles from Two Separate Missions to the International Space Station. npj Microgravity 5, 1. doi:10.1038/s41526-018-0061-0

Morrison, M. D., Fajardo-Cavazos, P., and Nicholson, W. L. (2017). Cultivation in Space Flight Produces Minimal Alterations in the Susceptibility of Bacillus subtilis Cells to 72 Different Antibiotics and Growth-Inhibiting Compounds. Appl. Environ. Microbiol. 83 (21), e01584. doi:10.1128/AEM.01584-17

Nicholson, W. L., and Ricco, A. J. (2020). Nanosatellites for Biology in Space: In Situ Measurement of Bacillus subtilis Spore Germination and Growth after 6 Months in Low Earth Orbit on the O/OREOS mission. Life 10 (1), 1–14. doi:10.3390/life10010001

Nicholson, W. L., and Setlow, P. (1990a). Dramatic Increase in Negative Superhelicity of Plasmid DNA in the Forespore Compartment of Sporulating Cells of Bacillus subtilis. J. Bacteriol. 172 (1), 7–14. doi:10.1128/jb.172.1.7-14.1990

Nicholson, W. L., and Setlow, P. (1990b). "Sporulation, Germination, and Outgrowth," in Molecular Biological Methods for Bacillus. Editors C. R. Harwood and M. Cutting (New York: J. Wiley & Sons).

NRC (2011). Recapturing a Future for Space Exploration: Life and Physical Sciences Research for a New Era. Washington, DC: National Academies Press.

Rosenzweig, J. A., Ahmed, S., Eunson, J., and Chopra, A. K. (2014). Low-shear Force Associated with Modeled Microgravity and Spaceflight Does Not Similarly Impact the Virulence of Notable Bacterial Pathogens. Appl. Microbiol. Biotechnol. 98, 8797–8807. doi:10.1007/s00253-014-6025-8

Sadiq, R., Khan, Q. M., Mobeen, A., and Hashmat, A. J. (2015). In Vitro toxicological Assessment of Iron Oxide, Aluminium Oxide and Copper Nanoparticles in Prokaryotic and Eukaryotic Cell Types. Drug Chem. Toxicol. 38 (2), 152–161. doi:10.3109/01480545.2014.919584

Schaeffer, P., Millet, J., and Aubert, J. P. (1965). Catabolic Repression of Bacterial Sporulation. Proc. Natl. Acad. Sci. 54 (3), 704–711. doi:10.1073/pnas.54.3.704

Schindelin, J., Arganda-Carreras, I., Frise, E., Kaynig, V., Longair, M., Pietzsch, T., et al. (2012). Fiji: An Open-Source Platform for Biological-Image Analysis. Nat. Methods 9 (7), 676–682. doi:10.1038/nmeth.2019

Schultz, E. R., Zupanska, A. K., Manning-Roach, S., Camacho, J., Levine, H., and Paul, A. (2012). Testing the Bio-Compatibility of Aluminum PDFU BRIC Hardware. Gravit. Space Biol. 26 (2), 48–63.

Strempel, V., Knemeyer, K., Naumann d'Alnoncourt, R., Driess, M., and Rosowski, F. (2018). Investigating the Trimethylaluminium/Water ALD Process on Mesoporous Silica by In Situ Gravimetric Monitoring. Nanomaterials 8 (6), 365. doi:10.3390/nano8060365

Taft, B. S., Smith, S. M., and Moulton, J. (2014). Contact Angle Measurements for Advanced thermal Management Technologies. Front. Heat Mass Transfer 5 (6), 1–9. doi:10.5098/hmt.5.6

Wang, B., and Muir, T. W. (2016). Regulation of Virulence in Staphylococcus A : Molecular Mechanisms and Remaining Puzzles. Cel Chem. Biol. 23 (2), 214–224. doi:10.1016/j.chembiol.2016.01.004

Wells, B., McCray, R. H., Best, M. D., and Levine, H. G. (2001). "A Flight-Rated Petri Dish Apparatus Providing Two Stage Fluid Injection for Aseptic Biological Investigations in Space," in 31st International Conference on Environmental Systems, Orlando, FL, July 9–12, 2001 (SAE International). doi:10.4271/2001-01-2286

Wollman, A. P., Weislogel, M. M., Wiles, B., and Pettit, D. (2016). More Investigations in Capillary Fluidics Using a Drop Tower. Experiments in Fluids 57 (4), 1–17. doi:10.1007/s00348-016-2138-4

Wollman, A., and Weislogel, M. (2013). New Investigations in Capillary Fluidics Using a Drop Tower. Exp. Fluids 54 (4), 1499. doi:10.1007/s00348-013-1499-1

SUPPLEMENTARY MATERIAL

The Supplementary Material for this article can be found online at: https://www.frontiersin.org/articles/10.3389/frspt.2021.797518/full#supplementary-material